Power Constrained Electric Propulsion Missions to the Outer Planets

IEPC-2007-304

Presented at the 30th International Electric Propulsion Conference, Florence, Italy
September 17-20, 2007

K. Geurts*, C. Casaregola*, P.Pergola* and M. Andrenucci†
ALTA S.p.A, Via Gherardesca 5, 56121, Pisa, Italy

The presented study has analyzed the transfer characteristics of missions based on small, power constrained spacecraft that employ Electric Propulsion in combination with a powerful launcher, to the outer planets. Power requirements at these solar distances are fulfilled by a radioisotope thermoelectric generator and the required high launch energy is based on an existing launcher, avoiding the reliance on future performance developments. The Electric Propulsion is modeled considering constant electrical power with a large range of specific impulses. The implementation of a numerical optimization scheme enabled the computation of time optimized trajectories. The transfer strategies consisted out of two phases; a discretized initial coasting phase followed by a propulsion phase. The duration of the coasting phase strongly influences the final mass fraction and total transfer time. This enabled the formation of three-dimensional surfaces showing the mass fraction and transfer time trends as a function of initial mass, coasting duration and specific impulse. These results are presented for Neptune, Uranus and Saturn, characterizing the various spacecraft configurations and identifying the mission feasibility envelopes.

Nomenclature

a	= acceleration
C_3	= launcher excess energy
I_{sp}	= specific impulse
$\dot{m}$	= propellant mass flow rate
m_i - m_f	= initial and final spacecraft mass
P	= input power
r	= spacecraft heliocentric radius
r_{planet}	= planet heliocentric radius
t	= time
T	= thrust
T_{bal}	= ballistic coasting duration
u	= radial velocity component
v	= azimuthal velocity component
V_{SC}	= spacecraft heliocentric velocity at initial time
V_{Earth}	= Earth heliocentric velocity
β	= thrust angle
ΔV_{launch}	= launcher excess velocity
η	= thrust efficiency
μ	= Sun gravitational constant

*Ph.D. Student, Dep. of Aerospace Engineering, University of Pisa; Research Engineer, Alta S.p.A., Member AIAA.
†CEO Alta S.p.A.; Professor, Dep. of Aerospace Engineering, University of Pisa, Senior Member AIAA.

I. Introduction

THE promising potential to decrease outer planetary transfer times based on the development of small, power constrained spacecraft, has already been demonstrated in the past.[1–8] These studies combined a Radioisotope Thermoelectric Generator (RTG) and Electric Propulsion (EP) with a powerful launcher, developing novel transfer strategies for outer planetary exploration. This enables the design of outer planetary missions based on relatively small spacecraft, capable of delivering a high payload fraction to their destination. The higher efficiency of EP with respect to conventional chemical means results in much lower propellant mass requirements for the high ΔVs that are needed. These significantly lower propellant masses, combined with the small spacecraft concept, allow the usage of powerful launchers that provide a significant portion of the high required ΔV budget.

Initially this concept was described by Noble,[1] who identified the possibility to use a chemically provided impulse to place a small spacecraft into an Earth escape trajectory and EP to modify the spacecraft energy. Here, the spacecraft is placed into a low Earth orbit where an expendable chemical thrust delivers the required Earth escape energy. Based on this approach Noble[2] determined the optimal thrusting strategy, maximizing the payload, to consist out of three phases: thrust - coast - thrust, where during the initial thrust phase the spacecraft is accelerated and during the second decelerated and the trajectory circularized. Principal requirement for successful implementation of this strategy is the necessity for sufficient electrical power at Sun distances well beyond Mars, typically considered the boundary for solar arrays, which is resolved by consideration of an RTG.

Extending the work carried out by Noble, Oleson[4–7] described a different strategy assuming a more powerful launcher in order to avoid the initial acceleration phase. The spacecraft is directly placed on a highly elliptical or hyperbolic heliocentric transfer trajectory towards its destination. The EP is in this case exclusively used to decelerate and circularize the trajectory upon reaching the destination planet.

The objective of this study is to assess the feasibility of outer planetary transfer trajectories based on small spacecraft design, in a more detailed manner covering a large range of power and specific impulse combinations.

II. Mission Analysis Procedure

The principal objective of the mission analysis studies is to characterize the initial mass and specific impulse parameter range for the previously discussed transfer strategy. The two main constraints on mission design are the total transfer time and the required mass at the destination. To maintain a high degree of mission feasibility, which is an essential factor throughout the study, an existing powerful launcher has been selected based on which C_3 and mass performance has been determined.

For all destinations considered a constant RTG electrical power of 1kW is hypothesized, where recent studies[6] give the RTG specific mass as approximately 200kg/kW. This would require the allocation of approximately 200kg of the final mass to the power subsystem. In the transfer analysis, the effective mass at the destination is a function of the initial mass, which is in turn determined by the launcher C_3, the specific impulse and the coasting duration. Consequently, the final mass obtained by the optimization should cover all spacecraft subsystems and scientific payload.

As highlighted above and as a result of the constant electrical power, the required propellant mass is a function of specific impulse (I_{sp}) and thrusting duration. To cover an ample spectrum of thruster characteristics, specific impulse values in the range from 1500s to 4500s, with a discretized step of 500s, are investigated. The last parameter that influences the propellant mass requirement is the ballistic coasting phase duration, which moreover has a strong effect on total transfer time. The ballistic coasting duration (T_{bal}) is parameterized to examine its effect on the mission performance, where it has been varied by planet, from zero up to more than 10 years.

Based on the above discussed parameters a numerical scheme was implemented that performed a trajectory optimization, computing the optimal thrust angle to guide the spacecraft to a predefined final state, minimizing the required time. As a consequence the thruster is constantly on during the propulsion phases, maximizing the rate of change of spacecraft energy. The parameterized initial ballistic coasting duration thus serves as a control parameter, because for identical C_3 and I_{sp}, different final masses and transfer times are obtained under variation of T_{bal}.

The numerical routine computes time optimized transfers between a given initial state, a circular orbit

with 1AU radius, and a heliocentric orbit with orbital radius equal to the planet under investigation. This has been done for the three outermost planets: Neptune, Uranus and Saturn. The launcher C_3 range considered goes from 130 to 170km^2/s^2 having an associated initial mass from 860 to 480kg, respectively. This link between launch energy and spacecraft initial mass has been determined with reference to the American Atlas 551 with Star 48V upper stage,[9] which is shown in Table 1.

Table 1. Launcher Performance[9]

Launcher C_3 [km^2/s^2]	Initial Mass [kg]
130	860
140	740
150	660
160	580
170	480

III. Mathematical Models

The characteristics of the transfer problem together with the limitations of the optimization techniques required for a definition of the system dynamics in a polar reference frame. Following, the mathematical models and optimization techniques employed are discussed.

A. System Dynamics

The transfer analysis approach outlined in the previous section requires thrust vector optimization with an open final time, consequently, the location of the intersection between the destination planet and the spacecraft is not known a priori. Thus the equations of motion describing the spacecraft's heliocentric behaviour must provide for the possibility to define a final state, a heliocentric orbit, without fixing the location on this orbit at the final time.

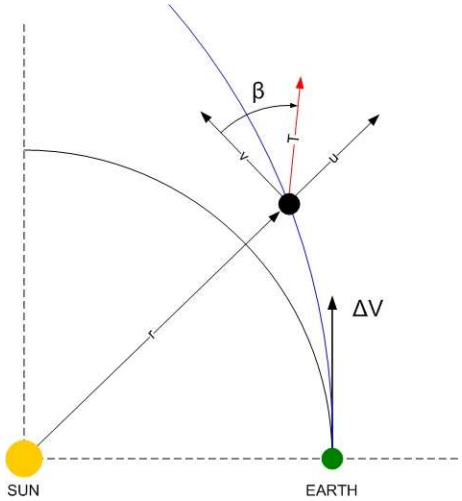

Figure 1. Definition of the System

Description of the equations of motion based on the radial distance, r, the angle, θ, the radial and azimuthal velocities, u and v respectively, solved this problem. Equations (1) describe the spacecraft dynamics in the aforementioned format, where the radial and azimuthal components have an additional accelerative term, representing the acceleration due to the thrust force.

$$\begin{cases} \dot{r} &= u \\ \dot{\theta} &= v \\ \dot{u} &= v^2/r - \mu/r^2 + asin(\beta) \\ \dot{v} &= -uv/r + acos(\beta) \end{cases} \tag{1}$$

Here a represents the acceleration which is given by the instantaneous values for power, specific impulse and spacecraft mass, as given in Eq. (2).

$$T = \frac{2\eta P}{g_0 I_{sp}} \quad \Rightarrow \quad a = \frac{T}{m_i - \dot{m}t} \tag{2}$$

The definition of the final state, a circular heliocentric orbit with radius equal to the orbital radius of the planet under investigation, can therefore be given as a function of the three state parameters at the final time, as shown in Eq. 3:

$$\begin{cases} r(t_f) &= r_{planet} \\ u(t_f) &= 0 \\ v(t_f) &= \sqrt{\mu/r_{planet}} \end{cases} \tag{3}$$

These final conditions will also serve to define the boundary conditions required by the optimization code, discussed in the next section. The spacecraft initial state, however, is a location on the Earth's orbit around the Sun. Due to the definition of the problem the exact location is not relevant as the model is symmetric. For all cases simulated the initial position is chosen as the right-side x-axis intersection, as seen in Fig. 1. The escape energy provided by the launcher ($\Delta V_{launch} = \sqrt{C_3}$) is added to the Earth's orbital velocity given by Eq. (4).

$$V_{SC} = V_{Earth} + \Delta V_{launch} \tag{4}$$

B. Optimization Techniques

The transfer from the end of the ballistic phase to the desired final orbit is computed using two different, supplementary, optimization techniques. Initially a gradient method is applied to provide a relatively accurate initial guess for a subsequently used forward shooting method. The latter method requires a precise initial guess of the initial state, which is obtained by the former, less sensitive, optimization scheme.

Both techniques are based on the calculus of variations where a control parameter, in this case the thrust angle, is varied to produce a stationary value of the defined functional, in this study the propulsion phase duration. The boundary conditions that must be satisfied are defined as the final state given in Eqs. (3).

The less sensitive *gradient method* requires an initial guess both for the thrust angle and the duration to achieve the final state. Based on these initial guesses the optimization code iterates the control parameter in order to obtain a stationary functional, which is achieved by varying the thrust angle in the direction of the negative (minimizing) gradient. Generally, the obtained solution sufficed as input for the much faster *forward shooting method*, which requires an initial guess for the spacecraft- and adjoint- state vector.

This combination of optimization techniques was able to provide a solution to all feasible scenarios investigated. The transfer optimization results are presented in the following section, all being obtained by the discussed approach.

IV. Mission Analysis

The mission analysis was done based on a stepwise procedure that leads to a parametric analysis to assess the mission characteristics for a given planet considering different initial masses, specific impulses and transfer strategies. This approach identifies a performance envelope that satisfies the typical mission constraints, transfer time and final mass, which form the basis for a more detailed trade-off analysis.

The procedure followed will be explained for a single case, where an identical procedure was followed for all other configurations, however, for brevity reasons this is omitted.

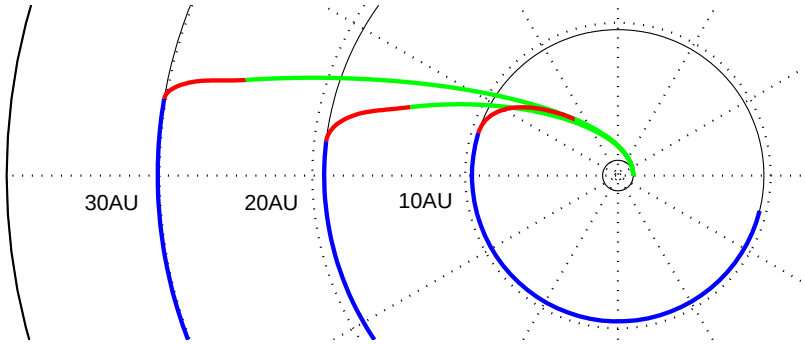

Figure 2. Typical geometry of the transfers with initial coasting (green), propulsion (red) and ballistic continuation (blue)

A. Uranus

The range of possible spacecraft configurations, initial mass - specific impulse combinations, for a single planet is given by the product of C_3 values and specific impulses, equating to a total of 35. For each of these configurations a different number of solutions exist governed by the number of parameterized ballistic coasting durations. This is not equal for all configurations as some m_i-I_{sp} combinations did not converge to a final state adhering the imposed boundary conditions for all ballistic durations. This emanated from the coasting phase being either too short or too long, consuming all available mass or not decelerating in time, respectively.

Figure 3 shows the results for the two extremes of launch energy, where the total transfer time and mass fraction are given as a function of different coasting durations and specific impulses. These are presented in three-dimensional figures for the two extremes of launch C_3. It is observed that for higher launch C_3, shorter coasting durations must be considered, especially for the higher specific impulses. The much larger excess energy transports the spacecraft towards its destination much faster, consequently for too long coasting durations the spacecraft is too close to its destination in order to decelerate and circularize the orbit.

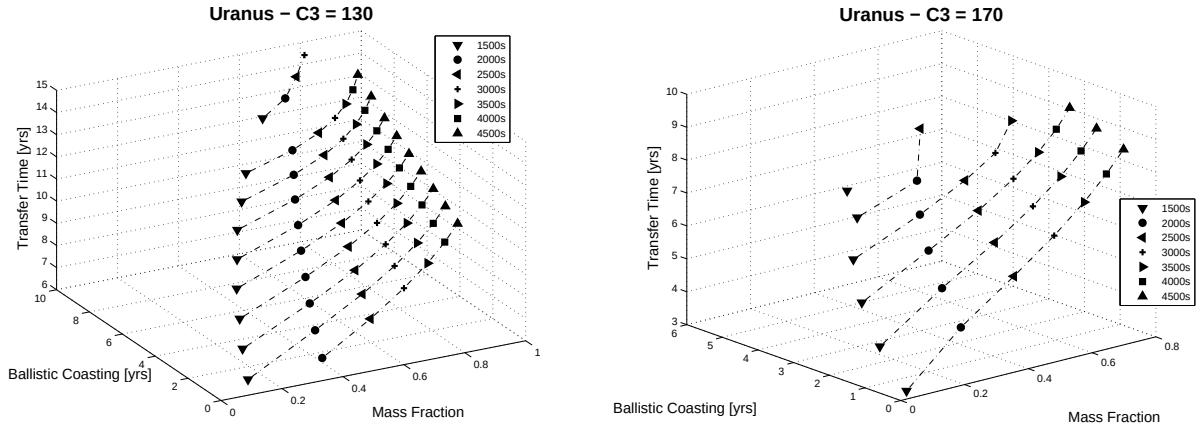

(a) Launch $C_3 = 130\text{km}^2/\text{s}^2$

(b) Launch $C_3 = 170\text{km}^2/\text{s}^2$

Figure 3. Transfer Time and Mass Fraction for Different Launch Energy

The strong vertical shift in transfer time for the $C_3 = 170$ case, between $I_{sp} = 2000$ and $I_{sp} = 2500$ is caused by the spacecraft trajectory going beyond the final radius before circularizing onto the specified heliocentric orbit, which results in a strong increase in transfer time.

Figure 4 shows two projections of the three-dimensional surface from Fig. 3a, presenting the total transfer time and mass fraction as a function of coasting duration only. It is observed that for the lowest I_{sp} value a coasting duration of 1 year is taken as minimum. The low I_{sp} value and short coasting duration result in a

very large propellant mass fraction. To minimize the transfer time the optimal trajectory has a long initial phase in which the thrust is mainly accelerating the spacecraft. Consequently the propellant mass fraction becomes very large, where in the extreme case this becomes unity. Higher I_{sp} values do not demonstrate this problem therefore coasting durations starting from zero years are also included.

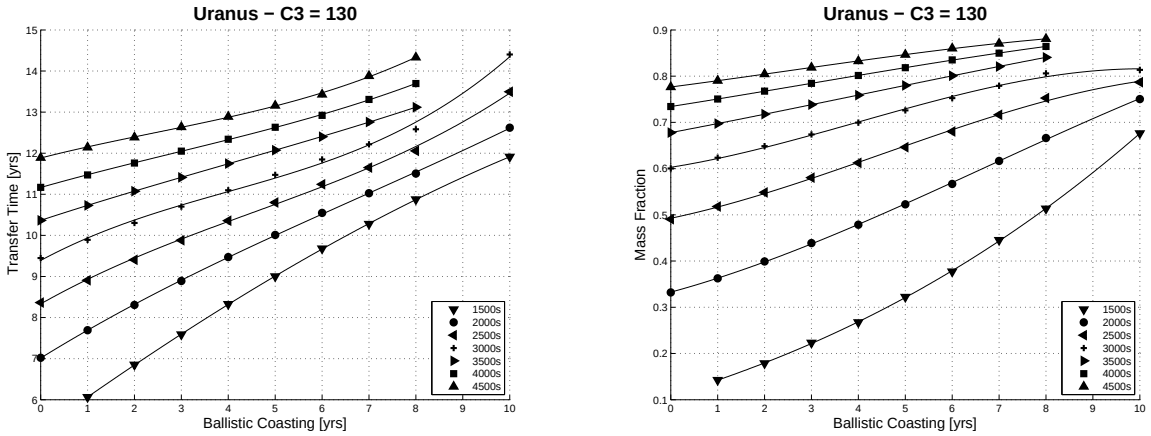

(a) Transfer Time

(b) Mass Fraction

Figure 4. Transfer Time and Mass Fraction for various Specif Impulses

An upper bound on the coasting duration is observed for the higher I_{sp} values. For longer durations the thrust force is no longer able to decelerate in time guiding the spacecraft towards the imposed boundary conditions. The higher I_{sp} values, for constant power, result in a lower thrust force, therefore more time is necessary to dissipate the excess energy.

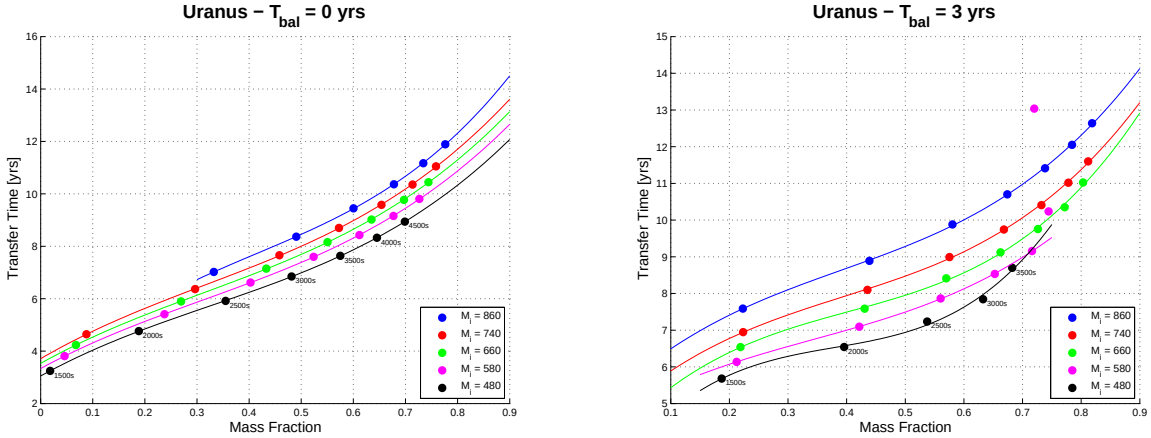

(a) Zero Ballistic Years

(b) Three Ballistic Years

Figure 5. Transfer Time versus Mass Fraction for Different Coasting Durations

A third order polynomial fit is applied to the computed data to obtain the trend lines. It is directly observed that a lower coasting duration results in a lower total transfer time, with the obvious mass fraction payoff. The transfer time decreases as the transfer includes an initial acceleration phase. As a result, increasing the coasting duration significantly increases the payload mass fraction, especially for the lower specific impulses. Moreover, in Fig. 4b, it can be seen that the variation in mass fraction for subsequent specific impulses decreases with increasing I_{sp} for a constant coasting duration. To maximize the mass fraction for a given value of specific impulse, a coasting duration that does not cause the spacecraft to go beyond the final radius, should be considered.

Figure 5 shows the results obtained for all initial masses considered and all specific impulses that lead

to a successful transfer, for equal coasting duration. Coasting durations of zero and three years are shown, where the colours represent the initial masses and the dots the specific impulses.

The figure showing no ballistic phase demonstrates a regular behaviour for the different initial masses and impulses. Whereas the three year coasting duration shows the vertical shift in transfer time, as mentioned previously. For the highest C_3 value the two highest specific impulses show a deviation from this behaviour, which results in the fit to bend upwards. This is explained by the spacecraft going beyond the final heliocentric radius before coming back. This effect is even more prominent for the $M_i = 560$kg case, where the $I_{sp} = 4000$s data point has been omitted for the data fit.

The zero coasting duration case is associated with the minimum total transfer time. When considering this for all evaluated initial masses, as given in Fig. 5a the performance envelope under certain mission constraints can be defined.

B. Neptune

A transfer analysis as described in the previous section is also performed for Neptune, considering identical launcher and thruster performance ranges, however, in this case the maximum coasting duration is augmented due to the much larger distance. For brevity reasons the two-dimensional figures showing the total transfer time and mass fraction as a function of the coasting duration are omitted. This is directly presented by the two three-dimensional figures for the extremes in launch energy, as seen in figure 6.

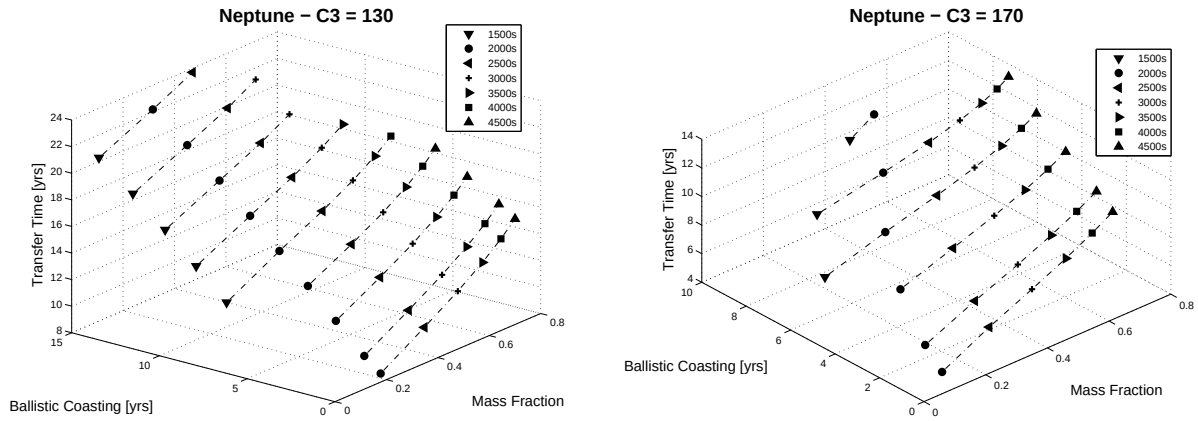

(a) Launch $C_3 = 130\text{km}^2/\text{s}^2$

(b) Launch $C_3 = 170\text{km}^2/\text{s}^2$

Figure 6. Transfer Time and Mass Fraction for Different Launch Energy

Trends similar to the Uranus case can be observed. The total transfer time increases with coasting duration, where this is accompanied with an increase in final mass fraction. This latter effect is more pronounced for the higher launch energies and lower specific impulses. Furthermore it is again observed that the lowest I_{sp} value has a minimum coasting duration significantly larger than the higher impulses and again the highest impulses are not capable to adhere the boundary conditions when considering long coasting durations. The overall shift in total transfer time and maximum coasting duration origin from the significantly larger Sun distance that must be reached.

Figure 7 shows the total transfer times versus the final mass fractions for zero and seven ballistic years, for all considered launch energies. It is seen that for none of the launch energies at zero ballistic time, a specific impulse of 1500s achieved the imposed final state. For the coasting duration of seven years, only the $I_{sp} = 4500$ case for the lowest launch energy did not manage to obtain a successful transfer.

It is clearly seen that the total transfer time always increases with specific impulse, for both coasting durations. However, for the shorter coasting durations, this increase in total transfer time, at constant specific impulse and different initial masses, goes together with an increase in mass fraction. The opposite behaviour is observed for longer coasting durations where the mass fraction actually decreases.

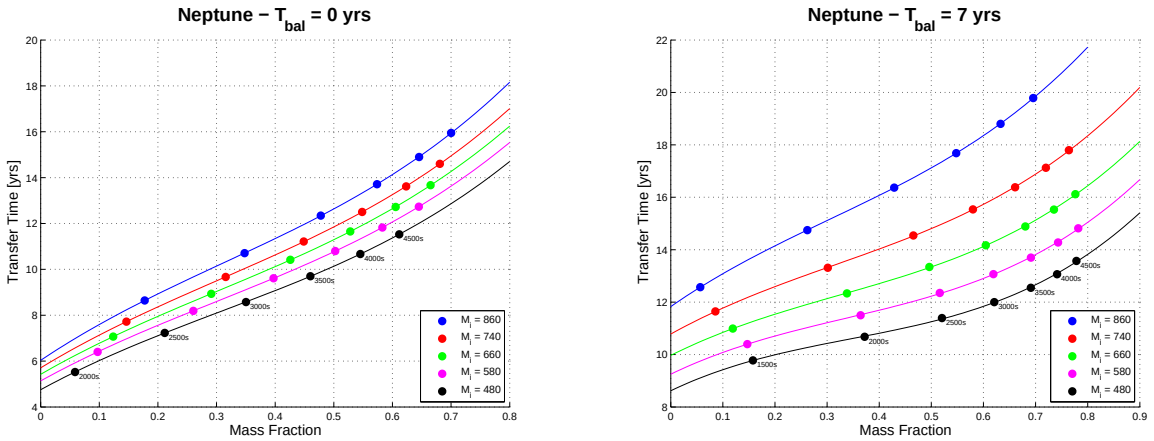

(a) Zero Ballistic Years

(b) Three Ballistic Years

Figure 7. Transfer Time versus Mass Fraction for Different Coasting Durations

C. Saturn

A transfer analysis as described in the previous sections is also performed for Saturn, considering identical launcher and thruster performances, however, the maximum coasting duration is strongly decreased to 1.5 years due to the shorter planetary distance. Figure 8 shows two three-dimensional surfaces giving the results for the two C_3 extremes.

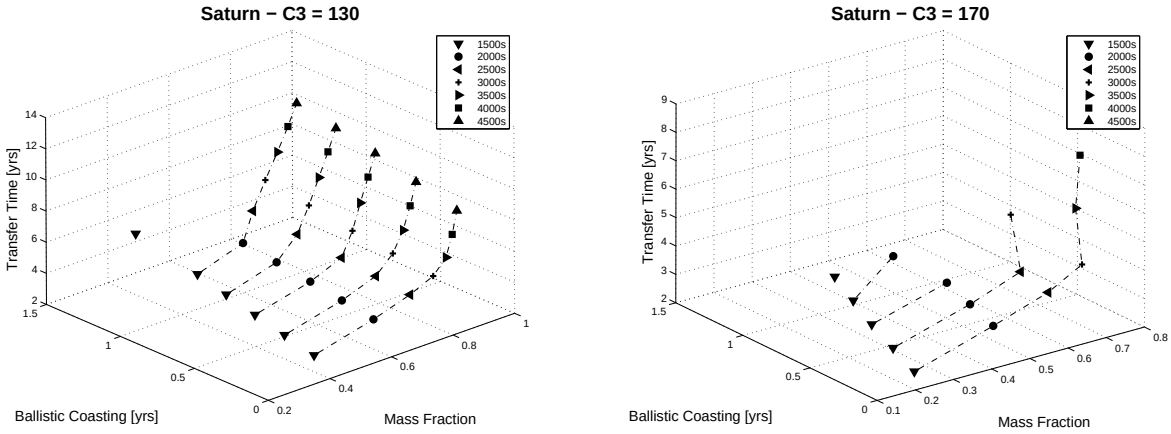

(a) Launch $C_3 = 130\text{km}^2/\text{s}^2$

(b) Launch $C_3 = 170\text{km}^2/\text{s}^2$

Figure 8. Transfer Time and Mass Fraction for Different Launch Energy

For Saturn a much more pronounced increase in total transfer time with increasing specific impulse can be observed. Especially for the higher launch energy, only the two lowest specific impulses are able to generate a deceleration high enough to satisfy the final conditions for coasting durations exceeding zero years. For the $C_3 = 170$ case the vertical shift in transfer time with almost constant mass fraction for two higher specific impulses is again explained by the fact that the trajectory goes beyond the final radius, after which it returns inwards.

Figure 9 shows the total transfer times versus the final mass fractions for zero and 0.25 ballistic years, for all considered launch energies.

The results indicate that the investigated strategy is less advantageous for a small spacecraft destined for Saturn. The planetary distance and high excess energy result in an unfavourable combination of spacecraft mass and required specific impulse, computing to low final mass fractions. A possible alternative could be a

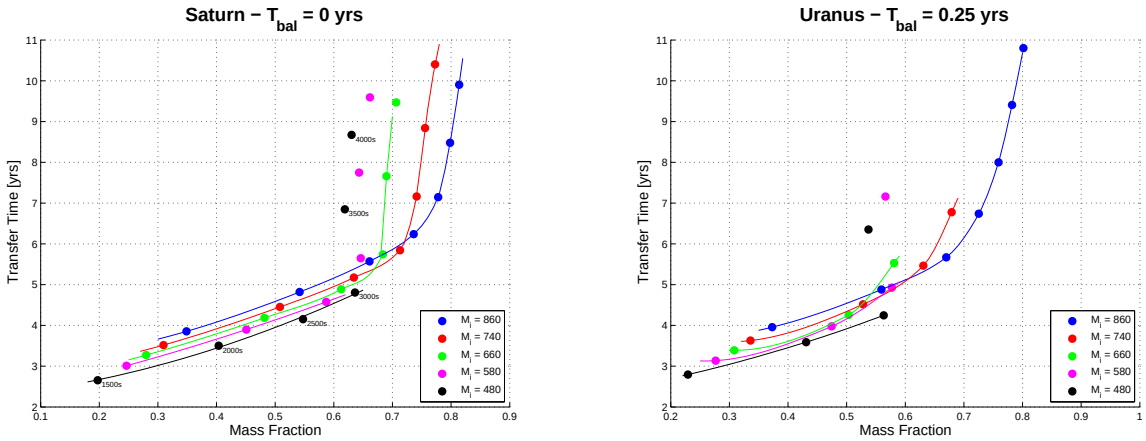

(a) Zero Ballistic Years

(b) Three Ballistic Years

Figure 9. Transfer Time versus Mass Fraction for Different Coasting Durations

less powerful launcher, providing the spacecraft with less excess energy, or considering the lower C_3 values investigated as these are not as susceptible to this behaviour. This tendency is also reported in previous studies,[7,8] suggesting a slightly different strategy for closer planets, associated with a less powerful launch.

V. Mission Design

Based on the presented results giving the transfer time and mass fraction as a function of the launch energy and specific impulse, a preliminary mission design can be performed. Typical parameters in feasibility studies are the maximum allowable transfer time and the minimum required final spacecraft mass. With respect to Fig. 5a this gives an upper bound on the transfer time and a point on the initial mass trends. These points for each initial mass can be connected producing the lower black line as seen in Fig. 10. This line gives the mass fraction for each initial mass, which corresponds with a final mass of 400kg. This final mass was randomly chosen for this example. The upper, horizontal black line represents the maximum allowable transfer time of 11 years.

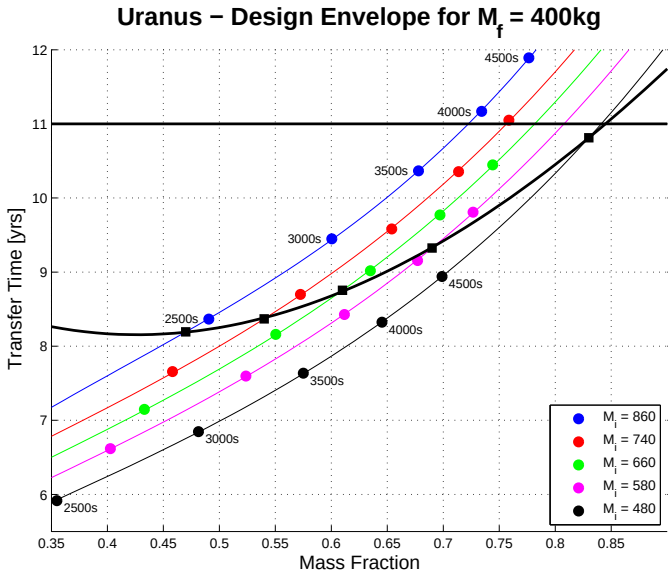

Figure 10. Design Envelope for 400kg Final Mass without a coasting phase ($T_{bal} = 0$)

The upper and lower bounds form the design space identifying the initial mass - specific impulse combinations that transport *at least* the minimum required final within the maximum allowable time. As seen, the highest initial mass with specific impulse of approximately 2500s meets these conditions in the minimum total transfer time. Based on this figure mission trade-off can be evaluated, for example, the effect of a different specific impulse on transfer time and final mass. In the case that no configuration provides a solution within the final mass bounds, different coasting durations must be evaluated providing higher final mass fractions. Consequently the total transfer times augment as well, therefore if still no satisfactory combination is identified, no transfer solution exists for the investigated parameter range.

VI. Conclusion

This study has investigated and outlined the characteristics of different spacecraft configurations with respect to outer planetary missions. A particular spacecraft configuration is identified by the initial mass and specific impulse for a constant power. The investigated transfer strategy comprising a high energy launch, an initial coasting phase and subsequent application of a low thrust to steer the spacecraft to a predefined final state, is based on the existing high performance Atlas 551 launcher.

This investigated strategy proved very promising for the two outermost planets, Uranus and Neptune, taking a small spacecraft to its destination in acceptable transfer times and with considerable mass fractions. Evaluation with respect to Saturn showed limitations due to the closer planetary distance, requiring lower specific impulses and lower initial launch energies in order to decelerate the spacecraft in time.

With respect to previous studies, the current work does not merely give a single transfer for each planet with a parameterized final mass, stating optimal specific impulses, but enables the investigation of the mass fraction and transfer times trends for different specific impulses and coasting durations. This defines a feasibility envelope giving the possible parameter ranges, which can assist during preliminary mission studies. Based on final mass and total transfer time constraints the presented data directly shows what initial mass and specific impulse combinations are capable to perform the transfer.

References

[1]R.J. Noble, *Radioisotope Electric Propulsion of Small Payloads for Regular Access to Deep Space*, AIAA 93-1897, 29th Joint Propulsion Conference, Monterey, California, 1993

[2]R.J. Noble, *Radioisotope Electric Propulsion for Small Robotic Space Probes*, British Interplanetary Society 49, pp 445-468, 1996

[3]R.J. Noble, *Radioisotope electric propulsion of science-craft to the outer Solar System and near-interstellar space*, Proceedings 2nd IAA Symposium on Realistic Near-Term Advanced Scientific Space Missions, June 1998 Aosta (Italy), FERMILAB-Conf-98/231, August 1998.

[4]S.R.Oleson, S. Benson, L. Gefert, M. Patterson,J. Schreiber, *Radioisotope Electric Propulsion for Fast Outer Planetary Orbiters*, AIAA-2002-3967, 38th Joint Propulsion Conference, Indianapolis, Indiana, July, 2002.

[5]S.R. Oleson, L. Gefert, M. Patterson, J. Schreiber, S. Benson, J. McAdams, P. Ostdiek, *Outer Planet Exploration with Advanced Radioisotope Electric Propulsion*, IEPC-2001-0179, 27th International Electric Propulsion Conference, Pasadena, California, October 2001.

[6]D.I. Fiehler, S.R. Oleson, *Radioisotope Electric Propulsion Missions Utilizing a Common Spacecraft Design*, IAC04IAA.3.6.4.01, International Astronautical Congress, October 2004 - Vancouver (Canada), NASA/TM2004-213357, Oct 2004.

[7]S.R. Oleson, D. Fiehler, *Mission Steering Profiles of Outer Planetary Orbiters Using Radioisotope Electric Propulsion*, NASA/TM-2004-212877

[8]C. Casaregola, K. Geurts, P. Pergola and M. Andrenucci, *Radioisotope Low-Power Electric Propulsion Missions to the Outer Planets*, AIAA-2007-5234, 43th Joint Propulsion Conference, Cincinnati, Ohio, July, 2007

[9]Lockheed Martin Corporation, *Atlas Launch System Mission Planner's Guide*, Revision 10a, January 2007